Scientific Research Publishing

American Journal of Plant Sciences, 2022, 13, 517-540
https://www.scirp.org/journal/ajps
ISSN Online: 2158-2750
ISSN Print: 2158-2742

Assessing Change of Lamto Reserve Area Based on the MODIS Time Series Data and Bioclimatic Factors Using BFAST Algorithms

Christian Jonathan Anoma Kouassi[1], Dilawar Khan[1], Lutumba Suika Achille[1], James Kehinde Omifolaji[2,3], Mikouendanandi Mouendo Rahmat Brice Espoire[4], Kebin Zhang[1], Xiaohui Yang[5*]

[1]School of Soil and Water Conservation, Beijing Forestry University, Beijing, China
[2]School of Ecology and Nature Conservation, Beijing Forestry University, Beijing, China
[3]Department of Forestry and Wildlife Management, Federal University Dutse, Dutse, Jigawa State, Nigeria
[4]School of Economics and Management, Beijing Forestry University, Beijing, China
[5]Institute of Desertification Studies, Chinese Academy of Forestry, Beijing, China
Email: anoma@bjfu.edu.cn, ctccd@bjfu.edu.cn, achille@bjfu.edu.cn, Dilawarafridi333@bjfu.edu.cn, omifolajijames@bjfu.edu.cn, mikimouendo@bjfu.edu.cn, *yangxh@caf.ac.cn

How to cite this paper: Kouassi, C.J.A., Khan, D., Achille, L.S., Omifolaji, J.K., Espoire, M.M.R.B., Zhang, K.B. and Yang, X.H. (2022) Assessing Change of Lamto Reserve Area Based on the MODIS Time Series Data and Bioclimatic Factors Using BFAST Algorithms. *American Journal of Plant Sciences*, **13**, 517-540.
https://doi.org/10.4236/ajps.2022.134034

Received: March 5, 2022
Accepted: April 26, 2022
Published: April 29, 2022

Abstract

Lamto Reserve area is a savannah landscape threatened by periodic drought, and anthropogenic activities leading to natural ecological imbalance. The ecological support services of the landscape had been significantly impacted by the grassland ecosystem. The Breaks for Additive Season and Trend Algorithms have been implemented in R to analyze the land cover/land use dynamic in relation to the climatic driver of Lamto forest from 2000 to 2020. We examine the vegetation state breaks using vegetation phenological patterns, and several time series including the Normalized Difference Vegetation Index and the Enhanced Vegetation Index, were studied utilizing Breaks for Additive Season and Trend. The findings indicate that the phenological changes in the vegetation in 2020 resulted from an increased temperature from (27.7˚C) to (32.17˚C), and a decrease in precipitation (71.75 millimeters). The analysis of variance ANOVA of the non-parametric Mann-Kendall test reveals a strong correlation between Precipitation/Evapotranspiration Grass ($p < -0.413$), Temperature/Evapotranspiration Grass ($p < 0.311$), and Temperature/Normalized Difference Vegetation Index ($p < -0.468$). The findings show that the breaks in vegetation detected by the Breaks for Additive Season and Trend Algorithms were caused by temperature extremes and reduced rainfall.

Keywords

Assessing, Break, Change Detection, Land Cover, Climate Extreme, Vegetation Vulnerability

1. Introduction

Savannah ecosystem represents approximately one-fifth of the world's land area and almost half of the African landscape [1] [2]. These environments occupy an important place in the ecosystems of tropical warm regions: cover vast areas in both the southern hemisphere and the northern hemisphere. Moreover, the relationship between the periodic passing of bushfires and the presence of trees and grasses has significant originality and poses biological problems for conservation and management. Savannahs are becoming increasingly important economically, as for many tropical ecosystems, in Africa, However, understand the principles that govern the use in agriculture, for animal husbandry. This theoretical and applied interest has revived research efforts in recent years, cumulating in several publications.

Nevertheless, literature savannah ecosystem is limited. These biocenoses provide a wide range of essential ecosystem services, including carbon sequestration, water recharge, soil stability, meat and dairy production, firewood, water supply and sanitation, tourism, and recreation [3]. Furthermore [4], African savannas have rich biodiversity and provide habitat functionality for migratory populations.

With the projected increase in these climate extremes as a result of future climate change [5], it is critical to have up-to-date information and knowledge of the severity and patterns of these ecological impacts, which become crucial because of extremes in terms of climate variables re not always associated with their result [6].

Nevertheless, the savannah ecosystems face degradation due to changes in land use, climate change, and stewardship regimes [7] [8].

However, in remote sensing, detection change can be defined as the difference between "two points in time", which can be discovered by comparing images of the same place taken at two different times [9]. Many authors addressed environmental change detection [10]-[15]. The unique advantage of remote sensing is that it allows monitoring the gradual and continuous changes [16] [17] over time [18].

A time series is a collection of images of the same area taken over time. These statistics assist us in understanding how environmental change happens in various ways, with varying causes and durations, for a more in-depth examination. These methods operate with time-series images by computing different characteristics per pixel and then incorporating these features into standard machine learning processes. Methods of bitemporal analysis attempt to identify and analyze differences between two observations. Image difference ratio [19] [20] and change vector analysis [21] are examples of methods. Other methods families are devoted to the study of image time series. The majority of them are based on a categorization that has evolved through time. One method examines radiometric trajectories [22]. These methods use time series analysis [23] to assess changes in the look of the ground over time (e.g., season, vegetation development [24] as well as the date sequence. There are many methods for analyzing data to identify patterns, and spectral analysis approaches are described in more detail below.

Recently, a new method for classifying remote sensing images and creating land cover maps has been explored. Random Forest, Artificial neural networks, BFAST, and other methods are examples of these methods.

According to [25], the application of the BFAST method boils down to the decomposition of image time series data for the detection of different types of structural changes and modifications (breakpoint) operated in the trend and seasonal components to pinpoint and identify changes in the land cover.

In recent years, several authors have become increasingly interested in land cover assessment, monitoring, and detection studies through the use of Moderate Resolution Imaging Spectroradiometer (MODIS) time series data [22] [26] [27] [28] [29] [30]. This method seems to be the most advantageous compared to the classical image processing technique based on a small number of images, usually two images on which the study is based. The BFAST algorithm methodology [22] [31]; is increasingly employed in almost all fields of environmental studies. This algorithm allows for better and more accurate detection of structural changes, especially in the detection of ecosystem disturbances such as droughts, fires, and vegetation changes [31] [32] [33]; in the agricultural [34] and forestry landscapes [35] [36].

Furthermore, [37] argues that the use of time series of long-term satellite imagery is suitable for assessing vegetation dynamics at the regional or even national scale. In addition, in the context of the climate crisis and significant socioeconomic challenges, the preservation and safeguarding of ecosystems remain essential issues. World Bank projects a 2˚C increase in average temperature by 2050, with varying rainfall and a 30cm rise in sea level along the coast. The consequences of this temperature rise can have severe consequences for ecosystems and make them vulnerable. Despite the importance of savannah ecosystems in maintaining and regulating biogeochemical cycles, it is essential to understand the origin of the disturbances in these environments and their evolution.

For this reason, this study chose the Lamto reserve and its surroundings as the ideal environment for this study. Many authors have shown that NDVI is essential for change detection [38] [39] [40], but only in savannah biomes. Aside from that, some research conducted by authors such as [41] [42] has found alterations in nutrient cycling in arid savannahs and grasslands, which lack the thick tree cover that saturates laser visual imaging signals. As a result, they discovered that ecosystem structure and function changes substantially impacted the normalized difference vegetation index (NDVI). Therefore, this study combines the BFAST algorithm, vegetation indices, and climate parameters to detect and explain changes within the study area. According to several studies, extreme weather events negatively influence savannah ecosystems [43] [44] [45] [46]. There is a food shortage in Africa, where savannah regions are very susceptible to extremes temperatures [47]. As a result, it is critical to monitor savannahs due to their vulnerability to the effects of climatic extremes and because savannahs contribute to the preservation of ecosystem services. The ability to detect changes using temporal imagery allows us to solve many problems that are not feasible with bi-

temporal analysis methods [48] [49]. Therefore, it is more than necessary to associate certain other factors with improving the understanding of changes.

As a result, the research hypothesis of this study is: if the savannah ecosystem has been well protected by the establishment of the reserve, with no significant change in vegetation cover (EVI or NDVI), but with considerable variation in seasonal phenology caused by bioclimatic factors such as temperature and rainfall. This research aims to use the BFAST method to detect the sensitivity of tropical savannah vegetation indexes to the climatic extreme.

2. Material and Methods

2.1. Study Area

The Lamto Reserve was designated in 1998 as an integral biosphere reserve under the UNESCO label. The choice of this site is motivated by the fact that it is an essential nature reserve, an essentially herbaceous environment, and is

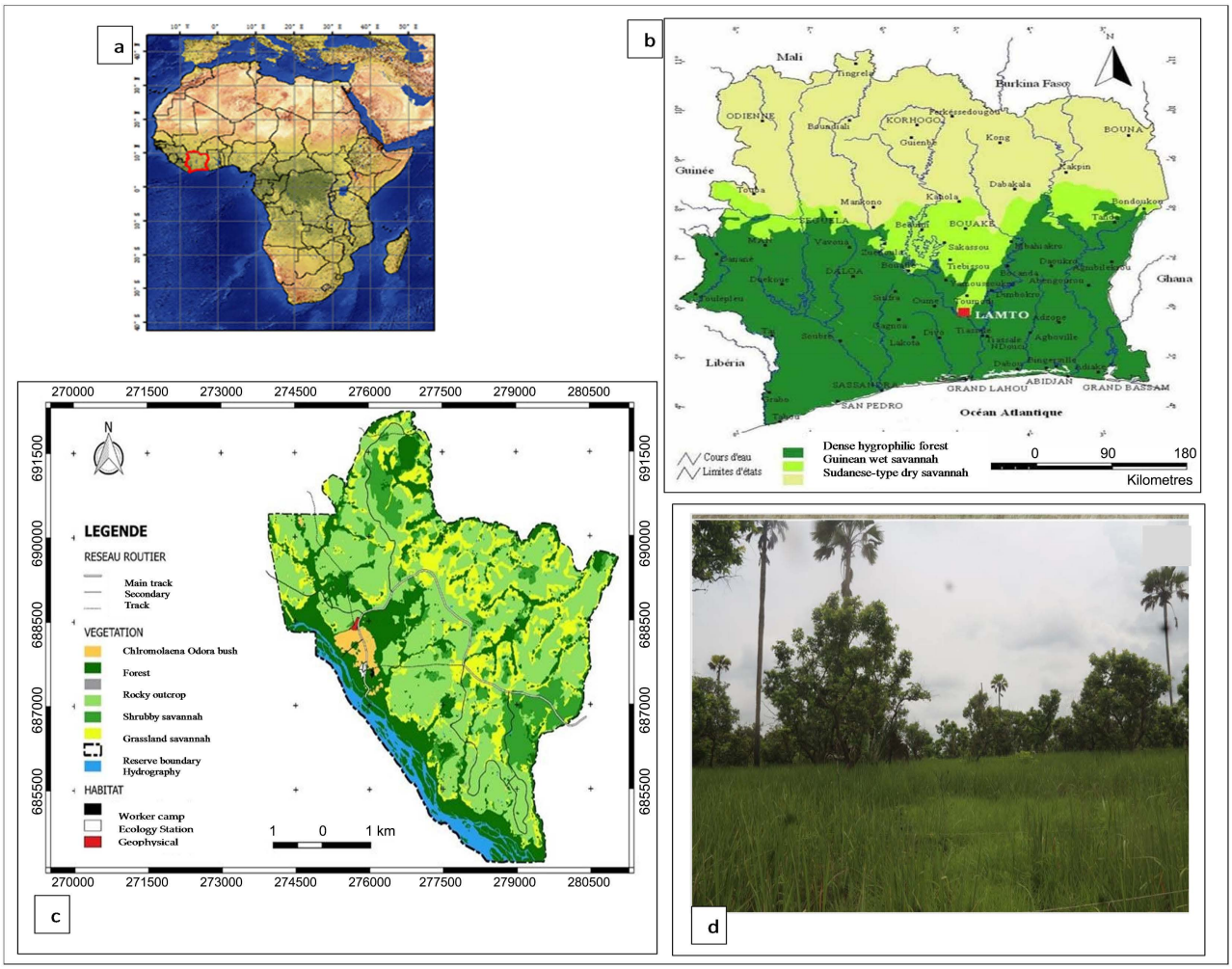

Figure 1. Illustrated maps of study area locations and plant species: (a) Map of Côte d'Ivoire showing the geographical location of the Lamto reserve [103] (within the red line) on the African continent; (b) location of the Lamto reserve (within the red line); (c) Vegetation map of the Lamto scientific reserve, Côte d'Ivoire (source: [104] digitized by [105]); (d) Guinean savannah [106].

situated in a region where natural herbaceous habitats exist, which are at least very stable and do not affect directly on human activity: such environments are rare, as we know. The savannah where the study is taking place belongs to the humid tropical zone of West Africa (**Figure 1**). This area is in the wilderness, where only the forest galleries are farmed, excluding the savannah. This area is located at the southern tip of the "V Baoulé", in the department of Taabo, in Cote d'ivoire (6˚9 à 6˚18N; 5˚15 à 4˚57E; http://lamto.free.fr/). It is located at the transition zone between forest and savanna woodland at the southernmost point of the "V Baoulé," the V-shaped incursion of savanna woodland into the forest belt in central Côte d'Ivoire [50] [51]. These forest fingers permeate the savanna woodland, which occupies the majority of the site. A conspicuous and typical element is the *Borassus* palm *Borassus aethiopum* which dominates the open shrubby woodland [52]. Typical grasses include *Loudetia simplex* and *Hyparrhenia spp.* Perennial grasses dominate the herbaceous stratum of savannas. Approximately ten species of perennial grasses, mainly of the *Andropogoneae* family, coexist in this savanna zone [53]. The average annual rainfall is 1200 mm. It is distinguished by a four-season cycle consisting of a long rainy season from March to July, a short dry season in August, a short rainy season from September to November, and a long dry season from December to February.

2.2. Methods

BFAST Lite is a family algorithm of BFAST. It is much faster to use and can run on a more significant area/higher resolution data. In addition, the development version of the bfast package includes optimizations that make it twice faster than the current CRAN version (https://github.com/bfast2/bfast).

The study data were analyzed in the R software version 4.0.3 Open-Source, installed on Windows 10, 64-bit. MODIS data were downloaded and processed using the packages "strucchange", "zoo", "bfast", "raster", "leaflet", "MODIS-Tools". The data used in this study are MODIS products MOD13Q1. The study method used to detect the phenological sensitivity to extreme variations of climatic factors such as temperature, precipitation, and Evapotranspiration time series (https://app.climateengine.org/climateEngine). Through the Normalized Difference Vegetation Index (NDVI), Enhanced Vegetation Index (EVI) [55] [56]. We applied the BFAST Monitor algorithm combined with BFAST Lite and the NDVI time series of the MODIS 16-day data to determine the different changes in the study area, based mainly on the NDVI as an indicator of vegetation vigour [57] (**Figure 2**).

The MODIS satellite data that we used for detecting breaks in our times series study may be found on the MODIS Subsetting website (https://modis.ornl.gov/globalsubset/). MODIS data for particular places are available. We focus on the MOD13Q1 product, which consists of a 16-day global image with a spatial resolution of 250 m. Each image has multiple bands centered at 469, 645, and 858 nanometers for blue, red, and near-infrared reflectance. These bands are used to determine MODIS vegetation indices.

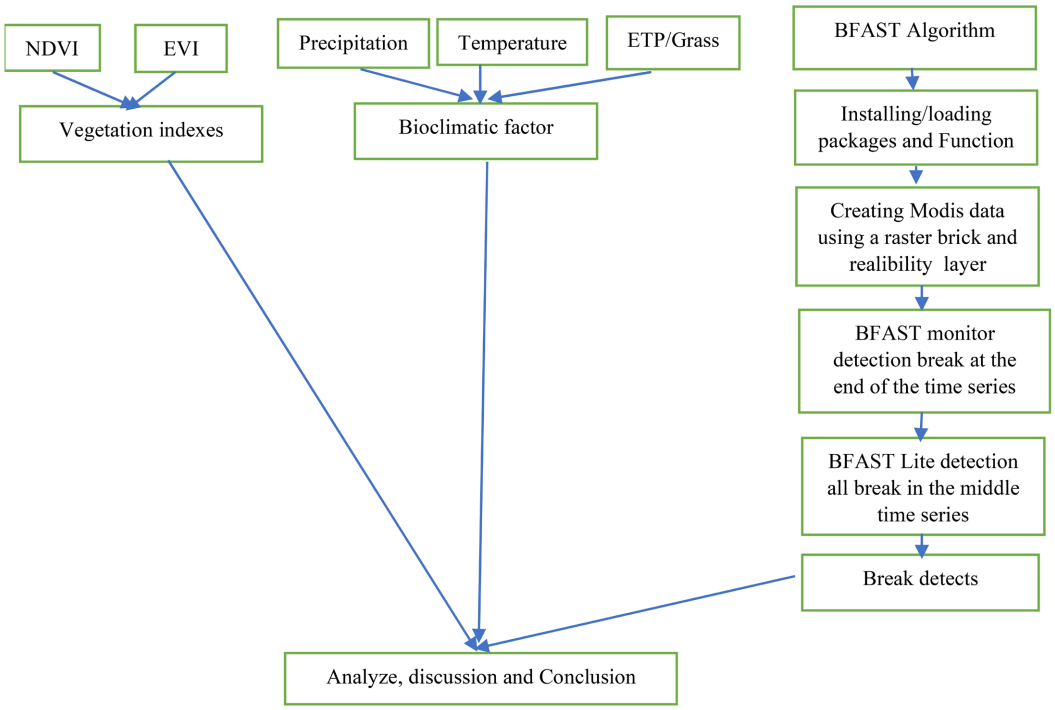

Figure 2. BFAST methodological workflow implemented in R.

Our choice to use vegetation indices such as NDVI and EVI for change detection is based on the fact that changes in these different biomes such as gallery forests, savannahs, grasslands can be amplified by NDVI and other vegetation indices compared to spectral values [58] [59]. For example, the time series of MODIS EVI was successfully used to classify land cover in China [60] [61] [62] [63]. Furthermore, studies by [64] confirmed that MOD13Q data have been widely used to monitor vegetation dynamics and determine trends and seasonal changes in satellite image time series [65] [66].

For our study, the rupture is detected inside the Lamto reserve, which has a surface area of 2500 ha and has been studied for 20 years.

2.2.1. Data

To measure the variation in phenological changes, we used MODIS NDVI data, product MOD13Q1, which are 16-day global images at 250 × 250 m spatial resolution acquired from January 2000 to December 2020 (**Table 1**) [56] [65] [66] [67].

2.2.2. Statistical Analysis

Statistical analyses were carried out on all the data collected using the regression method (Equation (1))

$$Y = ax + b \tag{1}$$

where Y dependent variable and x the independent variable; a and b are coefficient of regression used for determining provides the possibility to correlate the dependent and independent variants of the analysis series.

Table 1. Characteristics of data (https://modis.ornl.gov/).

Data	Satellite	Products	Day	Resolution
MODIS	NDVI	MOD13Q1	16	250 m
MODIS	EVI	MOD13Q1	16	250 m
MODIS	Evapotranspiration	MYD16A2	8	500 m

2.2.3. Statistics Nonparametric Mann Kendall (MK)

The nonparametric Mann Kendall time series trend test is recommended by [68] [69] was used to identify potential trends in the series of bioclimatic factors in the Lamto area during twenty years of study.

Two non-parametric analyses (MK) and (P) were performed with the following steps: the observed data in year Y_j and Y_i respectively differ, and the $sign(Y_j - Y_i)$ is equal to 1, −1, or 0 due to $j > i$. The test statistic, S, was then calculated (Equation (2)).

$$S = \sum_{i-1}^{n-1} \sum_{n=j-1}^{n} Sign\left(Y_j - Y_i\right) \tag{2}$$

If S is a more significant positive integer, the later values measured will be higher than the earlier values, and an upward trend is observed. When S is a more significant negative number, subsequent values tend to be smaller than previous values, indicating a downward trend. When the absolute value of S is small, no trend is shown. The test static τ was calculated (Equation (3)).

$$\tau = \frac{S}{n(n-1)/2} \tag{3}$$

when τ is between −1 and +1 and is similar to the correlation coefficient in the regression analysis. When the null hypothesis of no trend is rejected, S and τ are significantly different from zero. If a significant trend is found, the rate of change can be calculated using the slope estimator Sen (Equation (4)).

$$\beta = median \frac{Y_j - Y_i}{X_j - X_i} \tag{4}$$

For all $i < j$ and $i = 1, 2, \cdots, n-1$ and $j = 2, 3, \cdots, n$; in other words, calculate the slope for all pairs of data used to calculate S. The median of these slopes is the slope estimator Sen slope estimator. For [68] the S statistic is substantially within the norms if and only if the time range is more significant than eight. When there is no equality between the values of the data, see Equations (5) and (6).

$$E(S) = 0 \tag{5}$$

$$Var = \frac{n(-n)(2n+5)}{18} = \sigma \tag{6}$$

The standard test statistic Z is calculated according to the following equation:

$$Z = \frac{S-1}{\sqrt{Var(S)}} \quad \text{for } S \geq 0 \tag{7}$$

$$Z = 0 \quad \text{for } S = 0 \tag{8}$$

$$Z = \frac{S+1}{\sqrt{Var(S)}} \quad \text{for } S \le 0 \tag{9}$$

When there is no trend or null hypothesis in the analysis, the variable Z evolves with a mean of zero. When the p-value of Z is positive, it indicates an upward trend, while a negative value indicates a downward trend. To determine the p-value of a Mann-Kendall S, we use the normal cumulative distribution function (Equation (10)) [70] [71].

$$P = 2\left[1 - \phi\left(|z|\right)\right] \tag{10}$$

3. Results

Figure 3 shows the behavior of the NDVI of the area on day 2000-02-18. The graph analysis reveals that the BFAST algorithm did not identify a break within the vegetation in the period. Figure 4 shows the break detection in the vegetation 16-day NDVI image time series in one study area. The graph shows a slight change in vegetation phenology. The pixel value changes from green to yellow. Graph 1 is the quality control mask; it has the value "1" in areas with good data "0".

Figure 4 shows the timing of the break-up. This figure showed when the breaks were detected at the end of 2020 for each pixel in the study area. The vegetation structure of the site is homogeneous. The consequences of such extremes can have abrupt changes in the vegetation cover, but their effect is still unknown for a very long time.

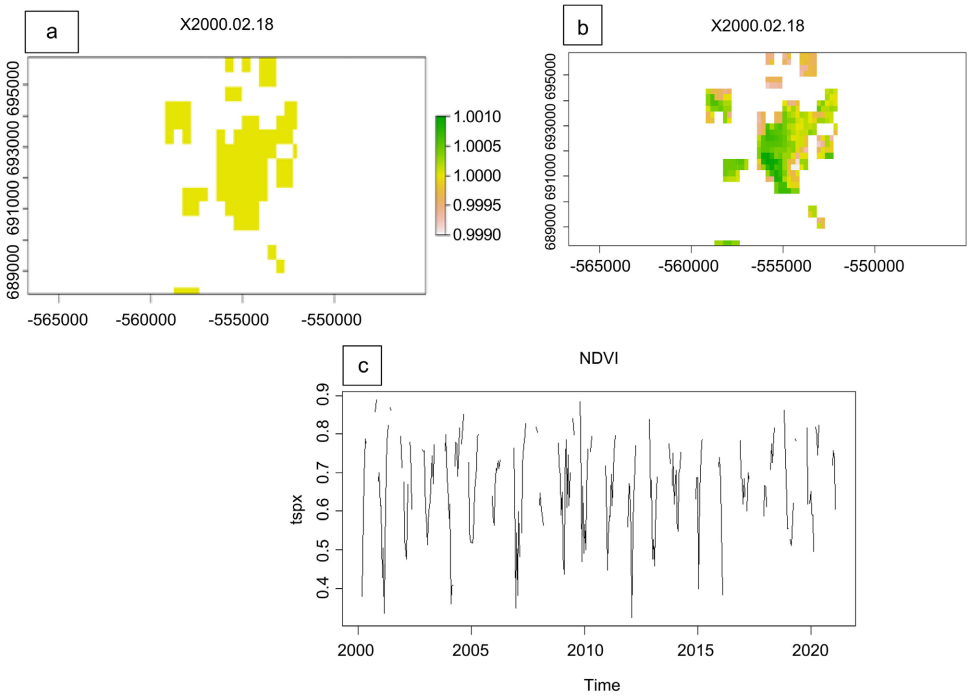

Figure 3. Automatic break detection (a) and (b): NDVI index, which captures the amount of green vegetation for a given target pixel/region; (c): NDVI time series of a particular pixel.

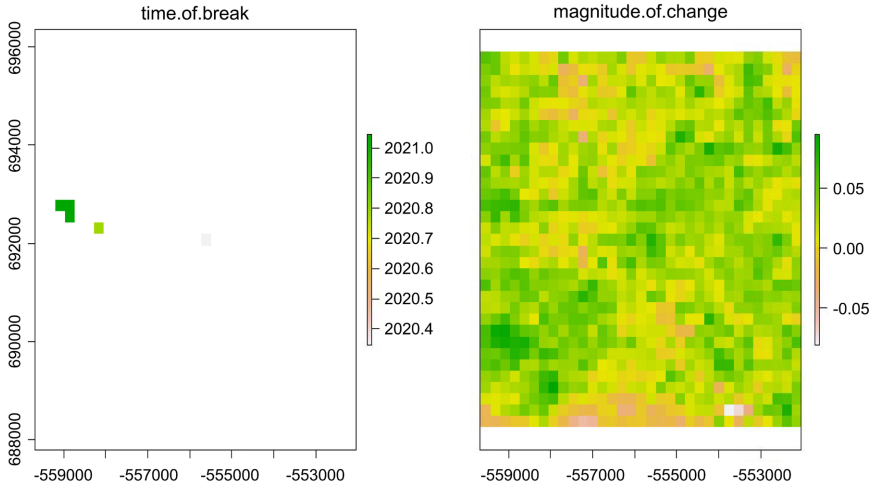

Figure 4. Timing of long-term phenological changes detected Break in MODIS NDVI images time (2000-2020) in Lamto reserve area.

The examination of the whole time series shows that in graph 5, the values reflect the state of the vegetation. The BFAST lite algorithm has identified a break in the research period. Throughout the study, the BFAST analyst was unable to detect any break in vegetation. The exact period indicated is at the end of the year, with pixel values between 69,300 and 69,400. The observed change trend has an amplitude value between −0.05 and 0.05. This result depicts the transition from dark green to yellow. Based on the expression of the vegetation coloration, these unusual phenological changes are notable. These major phenological in the Lamto savannah area are expected to occur between August and October 2020. At the same time, the study area saw a decrease in yearly rainfall (71.74 mm of water) and from 27.7˚C to 32.79˚C below the average. Beginning in 2015, a significant anomaly in both precipitation and temperature (**Figure 5**) occurred in the study area, resulting in severe drought stress and increased evapotranspiration at this time (**Figure 6**). The inter-annual precipitation variation is still more or less high over the whole study area, which shows that sequences of drought and humidity influencing the environment sub-set of NDVI and EVI values are classified by year to determine the variations in the study area.

The study of (**Figure 5(a)**) shows that the values of the average annual rainfall. The year 2010 was the period with the highest rainfall (134.5 mm). The years 2016 and 2017 were years of reduced rainfall with (4.83 mm) and (5.58 mm) respectively ($y = -2.0681x + 4248$; $R^2 = 0.16$) before increasing and falling back to a level of 79mm of rainfall in 2020 over the observed ten years period. (**Figure 5(b)**) depicts average maximum and minimum temperatures of 32.79˚C and 27.7˚C, respectively. The hottest temperatures recorded throughout the study period were 32.17˚C in 2016, and 32.79˚C in 2020 representing extreme climatic. Temperatures decreased in 2004 (29.75˚C) and 2008 (27.7˚C), then levelled out and peaked in 2016 ($y = 0.051x - 70.935$; $R^2 = 0.09$). Because of the cold weather in 2004, the average ET Grass (**Figure 6**) dropped substantially in 2004 and increased in 2007 (130 mm) and 2017 (125 mm) in the study period.

The average NDVI dropped in 2002 (0.05) and in 2005 (0.35) and 2020 (0.4) (Figure 7(a)). For EVI, the average dropped, in 2002 (0.1), in 2004 (0.25) and 2009 (0.3) (Figure 7(b)).

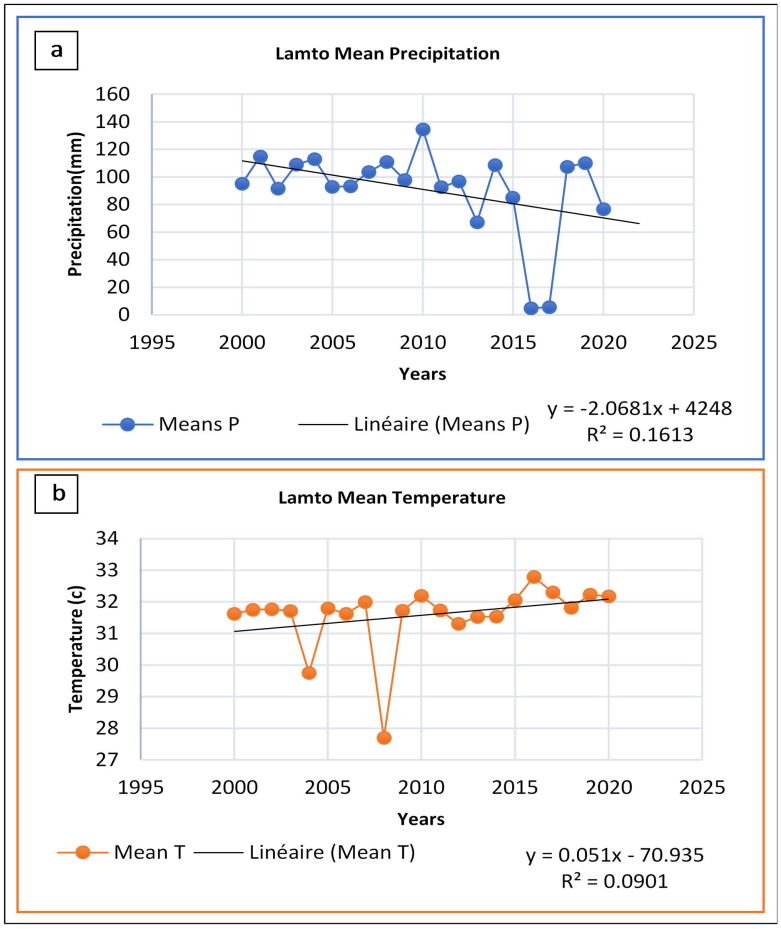

Figure 5. Climate factor time series (a): annual Temperature variations (˚C) and (b): annual precipitation variations (mm) in the study area.

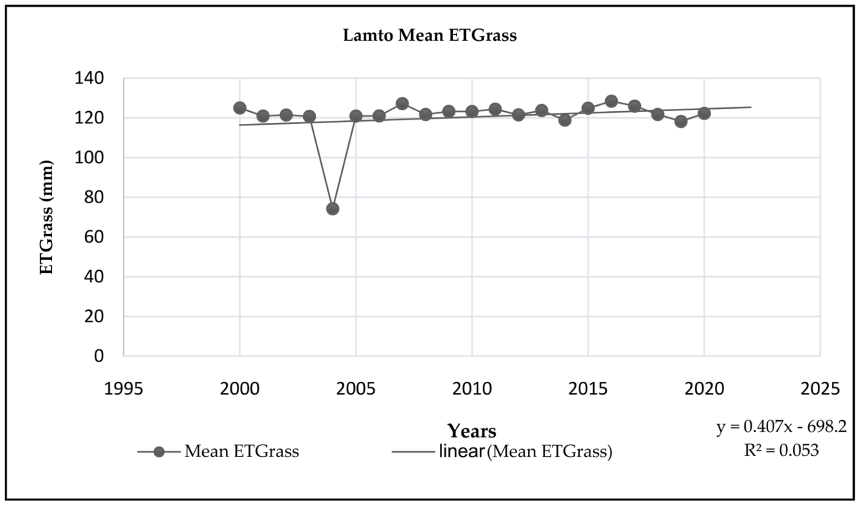

Figure 6. Time series of annual ETGrass variations (mm) in the study area.

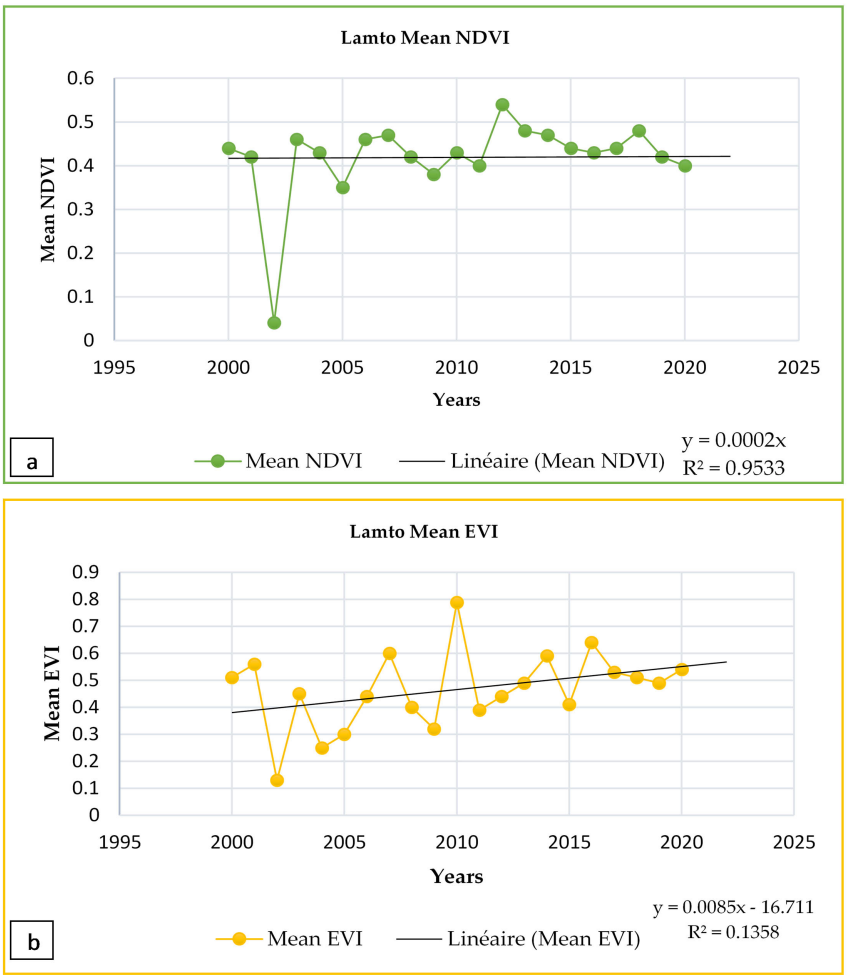

Figure 7. Time series of mean vegetation indexes in the study area (a): annual temperature variations (˚C) and (b): annual precipitation variations (mm).

Kendall's statistical analysis of the correlation table between the different parameters shows a negative correlation between precipitation and ET Grass at $p < 0.01$ with a coefficient of −0.413 (**Table 2**). There is a negative correlation between ET Grass and T at $p < 0.01$ and $p < 0.05$, respectively −0.413 and 0.311. There is also a positive correlation between T and ET Grass at $p < 0.05$ with a coefficient of 0.311. There is a negative correlation with a coefficient of −0.468 between Temperature and NDVI at $p < 0.05$. However, no correlation was found between the EVI and the climatic parameters.

The correlation between the NDVI and EVI values is almost similar. The NDVI trend is more pronounced than the EVI trend. The months of March, April, May, October, and November are the periods of strong growth in NDVI and EVI (**Figure 8(a)**, **Figure 8(b)**). However, the evolution remains constant over the whole study period (**Figure 9(c)** and **Figure 9(d)**). The decomposition of the subsets of NDVI and EVI indices by the MODIS sensor shows that within the study years, the months listed above are the months that are practically a dry season over the entire extent of the study area. Individually the months of

Table 2. Correlation analysis between bioclimatic factors and vegetation indexes.

			Precipitation	Temperature	ETGrass	NDVI	EVI
Kendall's tau_b	Precipitation	Correlation Coefficient	1.000	−0.162	−0.413**	0.000	0.020
		Sig. (1-tailed)		0.187	0.006	0.500	0.457
		N	21	21	21	21	21
	Temperature	Correlation Coefficient	−0.162	1.000	0.311*	−0.468*	0.201
		Sig. (1-tailed)	0.187		0.048	0.015	0.175
		N	21	21	21	21	21
	ETGrass	Correlation Coefficient	−0.413**	0.311*	1.000	−.016	0.306
		Sig. (1-tailed)	0.006	0.048		0.467	0.057
		N	21	21	21	21	21
	NDVI	Correlation Coefficient	0.000	−0.468*	−0.016	1.000	−0.194
		Sig. (1-tailed)	0.500	0.015	0.467		0.193
		N	21	21	21	21	21
	EVI	Correlation Coefficient	0.020	0.201	.306	−0.194	1.000
		Sig. (1-tailed)	0.457	0.175	0.057	0.193	
		N	21	21	21	21	21

**Correlation is significant at the 0.01 level (1-tailed). *Correlation is significant at the 0.05 level (1-tailed).

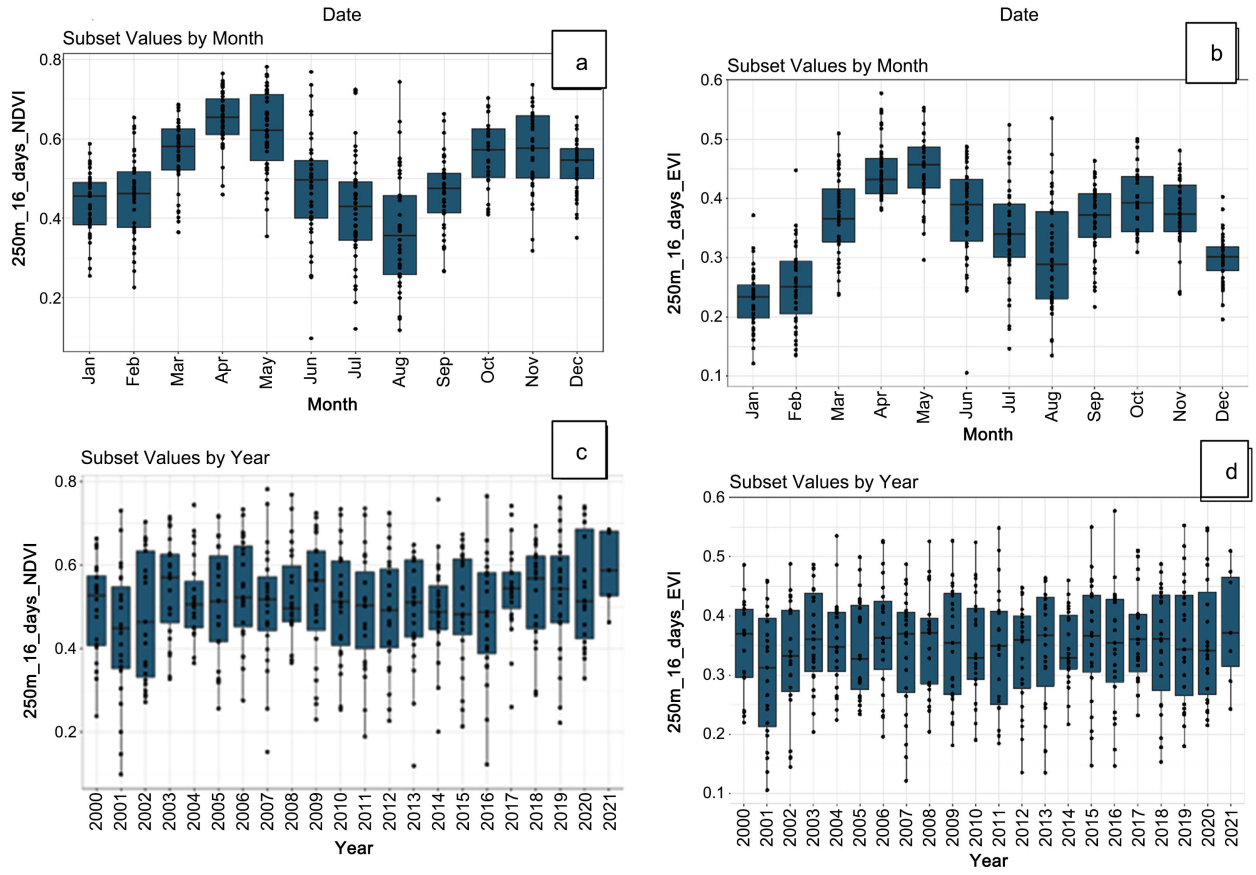

Figure 8. Trend of Vegetation indexes in the study area: (a) Variation in a subset of NDVI pixel means by month; (b) Variation in a subset of NDVI pixel means by month; (c) Variation in a subset of NDVI pixel means by year; (d) Variation in the subset of NDVI pixel means by year.

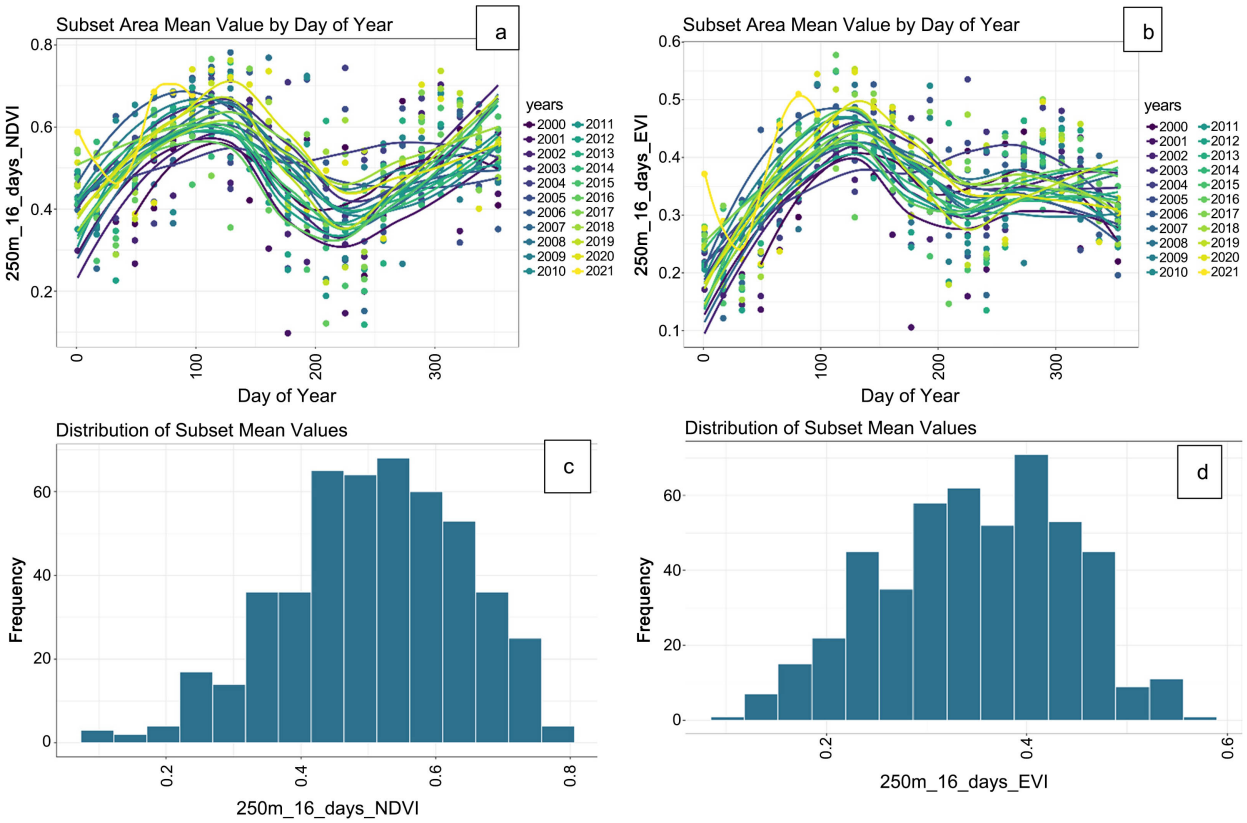

Figure 9. Dynamic of subset vegetation indexes: (a) Phenology dynamics of NDVI study area biomes by year; (b) Distribution of subset mean NDVI values; (c) Phenology dynamics of NDVI study area biomes by day; (d) Subset variation of NDVI pixel means by month.

the year taken separately, we record a significant decrease of about 0.38 of the NDVI of the vegetation during August (**Figure 8(a)**, **Figure 8(b)**), in contrast to the EVI, which shows the month of January as the lowest about 0.27. The two indices evolve in almost the same direction but with entirely different values.

The behavior of the vegetation about the NDVI and EVI indices over the whole study period shows that the trend of the two indices over the period differs slightly in the NDVI values (0.20) (**Figure 9(a)** and **Figure 9(b)**). In the study area, the subset of NDVI values distribution shows significantly higher frequencies than the EVI (**Figure 9(c)** and **Figure 9(d)**).

The behavior of the vegetation in the study area over the study period shows that there is a close relationship between NDVI and EVI. The correlation between NDVI and EVI in the study area indicates that EVI values are significantly lower than NDVI values. The comparative trend analysis of EVI and NDVI tells us that EVI is more sensitive to seasonal variation in biomass.

4. Discussion

Africa's grasslands and savannahs are considered hotspots of recent environmental change. According to the BFAST Lite findings, the breaks were discovered in 2020 (**Figure 4**). Indeed, the observed break in this time is the cause of

temperature extremes in the order of 32.79˚C in the year when the break was discovered. The natural ecosystem has suffered as a result of these temperature extremes. The extraneous detection pixels from multispectral satellite image data have values between 692,000 and 694,000. These results mean that this area has historically experienced very little ecological change from a disturbance point of view. The temperature time series analysis (**Figure 5(b)**) reveals that the high temperatures seen in 2002 had a detrimental impact on plant vigor and chlorophyll, resulting in a reduction in the NDVI and EVI values of the study region. Indeed, extreme temperatures impact climate extremes have a significant impact on plant vitality and sometimes lead to plant mortality [72]. The change is detected by BFAST (**Figure 4**) in 2020 revet and corresponds to climate extremes, which gives us insight into the underlying pattern of the vulnerability of such vegetation types [73]. This is the study's case; the primary concern in change detection studies is sometimes to detect the cause of the disturbance. Our research, which employs the BFAST algorithm, contributes to a better understanding of the study area's susceptibility and if high temperatures and other bioclimatic variables have influenced the vegetation of the Lamto reserve.

In addition to the use of BFAST, an analysis of the chronology of MODIS surface reflectance and ET series revealed that changes influenced these indices in climate parameters, namely the increase in temperature and decrease in precipitation during the study period. This has affected the vegetation's cover, causing its phenology to shift from green to yellow. A correlation between this severe change in vegetation and temperature has been established, elucidating the source of the shift as an increase in temperature of about 32.17˚C for a decrease in precipitation of 27 milimeters of water. These findings may be explained because the temperature rise has most likely resulted in a reduction in plant stomatal conductance and a decrease in vapor pressure, which influences plant NDVI. The change shown by the sensitivity of the NDVI and a reduction in the EVI at this time in the research region is irreversibly caused by a rise in temperature in the year 2020 when the record temperature was recorded. These two indicators represent the vitality of the vegetation at the research site and indicate the reduced perceptibility of changes [57]. This was readily identified by BFAST owing to its ability and capacity to identify the most sensitive seasonal changes within ecosystems as well as sudden changes in long-term patterns in greening and browning, as shown in our research [74] [75] [76] [77].

Indeed, the Lamto reserve is characterized by a savannah shrubland ecology. This ecosystem is very sensitive to temperature extremes, which influence the availability of water for plants and are the source of the reported break detection throughout the 2020 period. The relationship between temperature drops and rainfall is due to the unique characteristics of our study area, which is an ecological zone located at the forest/savanna interface (gallery forest, tree savanna, and grassland) and where annual, seasonal, intra-seasonal, inter-annual, and spatial changes in plant phenology in savannas, as well as variation within ecosystems, are not stable [78] [79]. This is quite logical, which is why this study explains

and highlights through the results of (**Figure 5**), that bioclimatic factors temperature and precipitation significantly influence vegetation changes in savannas [80] [81] [82]. Changes in climatic conditions have already been highlighted by [83] [84] [85] according to whom several changes have already been observed in the national climate, including decreasing and irregular rainfall, shorter rainy seasons, and a 0.5˚C warming of temperatures since the 1980s. These high temperature and low rainfall circumstances (**Figure 6(a)** and **Figure 6(b)**) will cause vegetative vulnerability.

The environment is dominated by three types of species, namely species with a herbaceous stratum, a shrub stratum, and a tree stratum [51], which are extremely sensitive to temperature rises and water stresses; this leads to vegetation senescence (NDVI) materialized by the drop in EVI, in the face of temperature rises and the reduction in the reference level of evapotranspiration.

Rising temperatures increase evapotranspiration (**Figure 5(b)** and **Figure 6**) of plants and wetlands in the Lamto area, which explains the positive relationship between mean annual temperature and evapotranspiration (**Table 2**) during specific periods of the study, most notably in the middle of 2010 and the last five years, which have been extremely hot and dry. Our results corroborate well with those studies [86], who claimed an energy exchange between the soil and the plant canopy due to plants consuming net radiation via the photosynthesis channel, which is transformed into evapotranspiration. Our findings indicate a link between evapotranspiration and temperature caused by solar radiation and the requirements of chlorophyllous plants for biosynthetic metabolic processes, as described by the authors [87] [88] [89]. Indeed, sunlight, temperature, and water availability significantly impact plant photosynthetic activities under all climatic conditions [90] [91] [92] resulting in plant vigor and productivity losses.

Using BFAST, we were able to combine and analyze NDVI pixels about climate parameters to identify impacts on environmental variability in savannah ecosystems and understand that extreme temperatures and decreasing precipitation can be a source of disturbance in African savannah ecosystems [93]-[102]. Bioclimatic extremes had a significant effect on the vegetation in the research region and were the source of the station wagon detections. The area's vegetation was influenced by a single event of rising temperatures and decreased precipitation in 2020. We can see that the rise in temperature and reduction in precipitation had a significant impact on the Lamto reserve. The algorithm and all of these factors work together to determine the precise moment of the break. The NDVI prediction values (**Figure 4**) were explained, identified, and perceived using BFAST. The vegetation change was predicted to be caused by an increase in temperature and a reduction in rainfall in the region. The correlation studies between the trends in land cover, NDVI/EVI; ETGrass; surface reflectance; and those observed in the detected precipitation and temperature, as well as the observed trend pattern, helped us understand and perceive that the vegetation change was caused by an increase in temperature and a decrease in precipitation in the area.

The BFAST method based on the detection of several breakpoints could not detect over one breakpoint. Based on the bioclimatic parameters, we note that within the inter-annual variation, decreases in rainfall patterns and increases in temperatures were observed, notably for rainfall in (2016: 4.83 mm), (2017: 5.58 mm) as well as for temperature in (2004: 29.75^{c}) and (2008: 27.7c). However, the BFAST lite algorithm could only detect one change and could not relate these inter-annual seasonal phenological variations to the study. Indeed, the method used in this study could not determine several breaks induced by the annual interactions between temperature and precipitation. But above all, the periodic variations because of the inter-annual variability of the climate [22].

5. Conclusions

The BFAST Lite approach was used in this work to analyze long-term patterns in vegetation response to bioclimatic variables. These have been used to explain changes brought about by external sources such as climate change. The establishment of the Lamto Reserve has had a significant role in the stewardship and conservation of the Lamto Ecological Zone. Over the entire study period, the only disturbance detected in the area was almost at the end of 2020. The BFAST Approach allowed seeing the most subtle change within the study period. Also, the vegetation index products from the MODIS sensor data, such as bioclimatic parameters (NDVI, EVI, ETGrass), revealed the seasonal phenological changes in the area and the cause of these changes. The BFAST algorithm allowed classifying the pixels by isolating the green and yellow pixels to mark the difference in the phenology of the vegetation in the study area. This BFAST detection allowed determining the exact disturbance over the study period and establishing the correlation between the temperature irregularities and the decrease in rainfall. The change detection within the Lamto area between increases in temperature from (27.7˚C) to 32.17˚C accompanied by a reduction in rainfall of 71.75 mm was marked by variation in seasonal phenology. Statistical analyses of the non-parametric Mann Kendall test and ANOVA revealed correlations between P/ETGrass ($p < -0.413$); T/ETGrass ($p < 0.311$); T/NDVI ($p < -0.468$), responsible for the variation in vegetation.

The explanation for this abrupt change could be found in the study of bioclimatic factors such as temperature, precipitation, and vegetation indices, which allowed us to understand that at the end of 2020, this area, had experienced an episode of rising temperature and falling precipitation. Inter-annual variability of African savannah biomass is strongly dependent on rainfall. This is advantageous for this area, a true ecological heritage that has undergone very little modification, allowing the conservation of ecosystem service functions and the regulation of the climate change phenomenon. The results obtained would be of great importance in that they could attract the attention of government authorities. This effort might aid in understanding the region's history and boost research on the carbon cycle, which would give a theoretical basis for environ-

mental planning and management as well as ecosystem services. This would help to preserve these ecosystems and predict potential harm.

Acknowledgements

This research was funded by China's International Science & Technology cooperation Programme and China's National Natural Science Foundation. We are also grateful to the Chinese and Coted'Ivoire Government for the cooperation scholarship for their generous help.

Conflicts of Interest

The authors declare no conflicts of interest regarding the publication of this paper.

References

[1] Ciais, P., Bombelli, A., Williams, M., Piao, S., Chave, J., Ryan, C., Henry, M., Brender, P. and Valentini, R. (2011) The Carbon Balance of Africa: Synthesis of Recent Research Studies. *Philosophical Transactions of the Royal Society A*: *Mathematical*, *Physical and Engineering Sciences*, **369**, 2038-2057. https://doi.org/10.1098/rsta.2010.0328

[2] Shackleton, C.M. and Scholes, R.J. (2011) Above Ground Woody Community Attributes, Biomass and Carbon Stocks along a Rainfall Gradient in the Savannas of the Central Lowveld, South Africa. *South African Journal of Botany*, **77**, 184-192. https://doi.org/10.1016/j.sajb.2010.07.014

[3] Solbrig, O.T. (1996) The Diversity of the Savanna Ecosystem. In: Solbrig, O.T., Medina, E. and Silva, J.F., Eds., Biodiversity and Savanna Ecosystem Processes, Springer, Berlin, Heidelberg, 1-27. https://doi.org/10.1007/978-3-642-78969-4_1

[4] Sankaran, M., Augustine, D.J. and Ratnam, J. (2013) Native Ungulates of Diverse Body Sizes Collectively Regulate Long-Term Woody Plant Demography and Structure of a Semi-Arid Savanna. *Journal of Ecology*, **101**, 1389-1399. https://doi.org/10.1111/1365-2745.12147

[5] O'Gorman, P.A. and Schneider, T. (2009) The Physical Basis for Increases in Precipitation Extremes in Simulations of 21st-Century Climate Change. *Proceedings of the National Academy of Sciences of the United States of America*, **106**, 14773-14777. https://doi.org/10.1073/pnas.0907610106

[6] Seneviratne, S., Nicholls, N., Easterling, D., Goodness, C.M., *et al.* (2012) Changes in Climate Extremes and Their Impacts on the Natural Physical Environment. In: Field, C.B., Barros, V., Stocker, T.F., Qin, D., Dokken, D.J. and Ebi, K.L., Eds., *Managing the Risks of Extreme Events and Disasters to Advance Climate Change Adaptation*, Cambridge University Press.

[7] Mitchard, E.T. and Flintrop, C.M. (2013) Woody Encroachment and Forest Degradation in Sub-Saharan Africa's Woodlands and Savannas 1982-2006. *Philosophical Transactions of the Royal Society B*: *Biological Sciences*, **368**, Article ID: 20120406. https://doi.org/10.1098/rstb.2012.0406

[8] Vogel, M. and Strohbach, M. (2009) Monitoring of Savanna Degradation in Namibia Using Landsat TM/ETM+Data. 2009 *IEEE International Geoscience and Remote Sensing Symposium*, Cape Town, 12-17 July 2009, III-931-III-934. https://doi.org/10.1109/IGARSS.2009.5417925

[9] Lhermitte, S., Verbesselt, J., Verstraeten, W.W. and Coppin, P. (2011) A Comparison

of Time Series Similarity Measures for Classification and Change Detection of Ecosystem Dynamics. *Remote Sensing of Environment*, **115**, 3129-3152. https://doi.org/10.1016/j.rse.2011.06.020

[10] Bell, R.L., Jarvis, K.G., Ottesen, A.R., McFarland, M.A. and Brown, E.W. (2016) Recent and Emerging Innovations in Salmonella Detection: A Food and Environmental Perspective. *Microbial Biotechnology*, **9**, 279-292. https://doi.org/10.1111/1751-7915.12359

[11] Bullock, J., Luccioni, A., Pham, K.H., Lam, C.S.N. and Luengo-Oroz, M. (2020) Mapping the Landscape of Artificial Intelligence Applications against COVID-19. *Journal of Artificial Intelligence Research*, **69**, 807-845. https://doi.org/10.1613/jair.1.12162

[12] Gross, J.E., Goetz, S.J. and Cihlar, J. (2009) Application of Remote Sensing to Parks and Protected Area Monitoring: Introduction to the Special Issue. *Remote Sensing of Environment*, **113**, 1343-1345. https://doi.org/10.1016/j.rse.2008.12.013

[13] Pham, T.D., Xia, J., Ha, N.T., Bui, D.T., Le, N.N. and Tekeuchi, W. (2019) A Review of Remote Sensing Approaches for Monitoring Blue Carbon Ecosystems: Mangroves, Sea Grasses and Salt Marshes during 2010-2018. *Sensors*, **19**, Article No. 1933. https://doi.org/10.3390/s19081933

[14] Bell, T.W., Allen, J.G., Cavanaugh, K.C. and Siegel, D.A. (2020) Three Decades of Variability in California's Giant Kelp Forests from the Landsat Satellites. *Remote Sensing of Environment*, **238**, Article ID: 110811. https://doi.org/10.1016/j.rse.2018.06.039

[15] Uhl, J.H. and Leyk, S. (2020) Towards a Novel Backdating Strategy for Creating Built-Up Land Time Series Data Using Contemporary Spatial Constraints. *Remote Sensing of Environment*, **238**, Article ID: 111197. https://doi.org/10.1016/j.rse.2019.05.016

[16] Alonso-Arévalo, M.A., Cruz-Gutiérrez, A., Ibarra-Hernández, R.F., García-Canseco, E. and Conte-Galván, R. (2021) Robust Heart Sound Segmentation Based on Spectral Change Detection and Genetic Algorithms. *Biomedical Signal Processing and Control*, **63**, Article ID: 102208. https://doi.org/10.1016/j.bspc.2020.102208

[17] Deng, C. and Zhu, Z. (2020) Continuous Subpixel Monitoring of Urban Impervious Surface Using Landsat Time Series. *Remote Sensing of Environment*, **238**, Article ID: 110929. https://doi.org/10.1016/j.rse.2018.10.011

[18] Vogelmann, J.E., Gallant, A.L., Shi, H. and Zhu, Z. (2016) Perspectives on Monitoring Gradual Change across the Continuity of Landsat Sensors Using Time-Series Data. *Remote Sensing of Environment*, **185**, 258-270. https://doi.org/10.1016/j.rse.2016.02.060

[19] Bruzzone, L. and Prieto, D.F. (2000) Automatic Analysis of the Difference Image for Unsupervised Change Detection. *IEEE Transactions on Geoscience and Remote Sensing*, **38**, 1171-1182. https://doi.org/10.1109/36.843009

[20] Jensen, J.R. (1981) Urban Change Detection Mapping Using Landsat Digital Data. *The American Cartographer*, **8**, 127-147. https://doi.org/10.1559/152304081784447318

[21] Johnson, R.D. and Kasischke, E. (1998) Change Vector Analysis: A Technique for the Multispectral Monitoring of Land Cover and Condition. *International Journal of Remote Sensing*, **19**, 411-426. https://doi.org/10.1080/014311698216062

[22] Verbesselt, J., Hyndman, R., Newnham, G. and Culvenor, D. (2010) Detecting Trend and Seasonal Changes in Satellite Image Time Series. *Remote Sensing of Environment*, **114**, 106-115.

https://doi.org/10.1016/j.rse.2009.08.014

[23] Bagnall, A., Lines, J., Bostrom, A., Large, J. and Keogh, E. (2017) The Great Time Series Classification Bake Off: A Review and Experimental Evaluation of Recent Algorithmic Advances. *Data Mining and Knowledge Discovery*, **31**, 606-660. https://doi.org/10.1007/s10618-016-0483-9

[24] Senf, C., Leitão, P.J., Pflugmacher, D., der Linden, S. and Hostert, P. (2015) Mapping Land Cover in Complex Mediterranean Landscapes Using Landsat: Improved Classification Accuracies from Integrating Multi-Seasonal and Synthetic Imagery. *Remote Sensing of Environment*, **156**, 527-536. https://doi.org/10.1016/j.rse.2014.10.018

[25] de Jong, R., Verbesselt, J., Schaepman, M.E. and De Bruin, S. (2012) Trend Changes in Global Greening and Browning: Contribution of Short-Term Trends to Longer-Term Change. *Global Change Biology*, **18**, 642-655. https://doi.org/10.1111/j.1365-2486.2011.02578.x

[26] Eklundh, L., Johansson, T. and Solberg, S. (2009) Mapping Insect Defoliation in Scots Pine with MODIS Time-Series Data. *Remote Sensing of Environment*, **113**, 1566-1573. https://doi.org/10.1016/j.rse.2009.03.008

[27] Galford, G.L., Mustard, J.F., Melillo, J., Gendrin, A., Cerri, C.C. and Cerri, C.E. (2008) Wavelet Analysis of MODIS Time Series to Detect Expansion and Intensification of Row-Crop Agriculture in Brazil. *Remote Sensing of Environment*, **112**, 576-587. https://doi.org/10.1016/j.rse.2007.05.017

[28] Jin, S. and Sader, S.A. (2005) MODIS Time-Series Imagery for Forest Disturbance Detection and Quantification of Patch Size Effects. *Remote Sensing of Environment*, **99**, 462-470. https://doi.org/10.1016/j.rse.2005.09.017

[29] Lunetta, R.S., Knight, J.F., Ediriwickrema, J., Lyon, J.G. and Worthy, L.D. (2006) Land-Cover Change Detection Using Multi-Temporal MODIS NDVI Data. *Remote Sensing of Environment*, **105**, 142-154. https://doi.org/10.1016/j.rse.2006.06.018

[30] Olofsson, P., Foody, G.M., Stehman, S.V. and Woodcock, C.E. (2013) Making Better Use of Accuracy Data in Land Change Studies: Estimating Accuracy and Area and Quantifying Uncertainty Using Stratified Estimation. *Remote Sensing of Environment*, **129**, 122-131. https://doi.org/10.1016/j.rse.2012.10.031

[31] Watts, L.M. and Laffan, S.W. (2014) Effectiveness of the BFAST Algorithm for Detecting Vegetation Response Patterns in a Semi-Arid Region. *Remote Sensing of Environment*, **154**, 234-245. https://doi.org/10.1016/j.rse.2014.08.023

[32] Hutchinson, J.S., Jacquin, A., Hutchinson, S.L. and Verbesselt, J. (2015) Monitoring Vegetation Change and Dynamics on US Army Training Lands Using Satellite Image Time Series Analysis. *Journal of Environmental Management*, **150**, 355-366. https://doi.org/10.1016/j.jenvman.2014.08.002

[33] Verbesselt, J., Zeileis, A. and Herold, M. (2012) Near Real-Time Disturbance Detection Using Satellite Image Time Series. *Remote Sensing of Environment*, **123**, 98-108. https://doi.org/10.1016/j.rse.2012.02.022

[34] Atzberger, C. (2013) Advances in Remote Sensing of Agriculture: Context Description, Existing Operational Monitoring Systems and Major Information Needs. *Remote Sensing*, **5**, 949-981. https://doi.org/10.3390/rs5020949

[35] Lambert, J., Drenou, C., Denux, J.-P., Balent, G. and Cheret, V. (2013) Monitoring Forest Decline through Remote Sensing Time Series Analysis. *GIScience & Remote Sensing*, **50**, 437-457. https://doi.org/10.1080/15481603.2013.820070

[36] Schmidt, M., Lucas, R., Bunting, P., Verbesselt, J. and Armston, J. (2015) Multi-Resolution Time Series Imagery for Forest Disturbance and Regrowth Monitoring

in Queensland, Australia. *Remote Sensing of Environment*, **158**, 156-168. https://doi.org/10.1016/j.rse.2014.11.015

[37] Schucknecht, A., Erasmi, S., Niemeyer, I. and Matschullat, J. (2013) Assessing Vegetation Variability and Trends in North-Eastern Brazil Using AVHRR and MODIS NDVI Time Series. *European Journal of Remote Sensing*, **46**, 40-59. https://doi.org/10.5721/EuJRS20134603

[38] Eisfelder, C., Klein, I., Niklaus, M. and Kuenzer, C. (2014) Net Primary Productivity in Kazakhstan, Its Spatio-Temporal Patterns and Relation to Meteorological Variables. *Journal of Arid Environments*, **103**, 17-30. https://doi.org/10.1016/j.jaridenv.2013.12.005

[39] Jacquin, A., Sheeren, D. and Lacombe, J.-P. (2010) Vegetation Cover Degradation Assessment in Madagascar Savanna Based on Trend Analysis of MODIS NDVI Time Series. *International Journal of Applied Earth Observation and Geoinformation*, **12**, S3-S10. https://doi.org/10.1016/j.jag.2009.11.004

[40] Li, X., Li, R., Li, G., Wang, H., Li, Z., Li, X. and Hou, X. (2016) Human-Induced Vegetation Degradation and Response of Soil Nitrogen Storage in Typical Steppes in Inner Mongolia, China. *Journal of Arid Environments*, **124**, 80-90. https://doi.org/10.1016/j.jaridenv.2015.07.013

[41] Prince, S.D. and Tucker, C.J. (1986) Satellite Remote Sensing of Rangelands in Botswana II. NOAA AVHRR and Herbaceous Vegetation. *International Journal of Remote Sensing*, **7**, 1555-1570. https://doi.org/10.1080/01431168608948953

[42] Eisfelder, C., Kuenzer, C. and Dech, S. (2012) Derivation of Biomass Information for Semi-Arid Areas Using Remote-Sensing Data. *International Journal of Remote Sensing*, **33**, 2937-2984. https://doi.org/10.1080/01431161.2011.620034

[43] Brown, D., Seymour, F. and Peskett, L. (2008) How Do We Achieve REDD Co-Benefits and Avoid Doing Harm? In: Angelsen, A., Ed., *Moving Ahead with REDD: Issues, Options and Implications*, Center for International Forestry Research, Bogor, 107-118.

[44] Meehl, G., Tebaldi, C. and Nychka, D. (2004) Changes in Frost Days in Simulations of Twentyfirst Century Climate. *Climate Dynamics*, **23**, 495-511. https://doi.org/10.1007/s00382-004-0442-9

[45] Merot, P., Delahaye, D., Desnos, P., Dubreuil, V., Gascuel, C., Giteau, J.-L., Joannon, A., Quénol, H. and Narcy, J.-B. (2014) Évaluation, impacts et perceptions du changement climatique dans le Grand Ouest de la France métropolitaine: Le projet CLIMASTER. *Cahiers Agricultures*, **23**, 96-107. https://doi.org/10.1684/agr.2014.0694

[46] Parry, M., Parry, M.L., Canziani, O., Palutikof, J., Van der Linden, P. and Hanson, C. (2007) Climate Change 2007-Impacts, Adaptation and Vulnerability: Working Group II Contribution to the Fourth Assessment Report of the IPCC. Vol. 4, Cambridge University Press, Cambridge.

[47] Vickers, N.J. (2017) Animal Communication: When I'm Calling You, Will You Answer Too? *Current Biology*, **27**, R713-R715. https://doi.org/10.1016/j.cub.2017.05.064

[48] Coppin, P., Jonckheere, I., Nackaerts, K., Muys, B. and Lambin, E. (2004) Review ArticleDigital Change Detection Methods in Ecosystem Monitoring: A Review. *International Journal of Remote Sensing*, **25**, 1565-1596. https://doi.org/10.1080/0143116031000101675

[49] Jianya, G., Haigang, S., Guorui, M. and Qiming, Z. (2008) A Review of Multi-Temporal Remote Sensing Data Change Detection Algorithms. The International Archives of the Photogrammetry. *Remote Sensing and Spatial Information Sciences*, **37**, 757-762.

[50] Lachenal, G. (2005) L'invention Africaine De L'écologie Française. Histoire De La Station De Lamto (Côte D'Ivoire), 1942-1976. *La Revue Pour L'histoire Du CNRS*, No. 13.

[51] Abbadie, L. and Menaut, J.-C. (2006) Geology, Landform, and Soils. In: Abbadie, L., Gignoux, J., Le Roux, X. and Lepage, M., Eds., *Lamto*, Springer, New York, 15-24. https://doi.org/10.1007/978-0-387-33857-6_2

[52] Vuattoux, R., Konaté, S., Abbadie, L., Barot, S., Gignoux, J. and Lahoreau, G. (2006) History of the Lamto Ecology Station and Ecological Studies at Lamto. In: Abbadie, L., Gignoux, J., Le Roux, X. and Lepage, M., Eds., *Lamto*, Springer, New York, 1-12. https://doi.org/10.1007/978-0-387-33857-6_1

[53] Abbadie, L., Gignoux, J., Roux, X. and Lepage, M. (2006) Lamto: Structure, Functioning, and Dynamics of a Savanna Ecosystem. Vol. 179, Springer Science & Business Media, New York. https://doi.org/10.1007/0-387-33857-8

[54] Jiang, Z., Huete, A. R., Didan, K. and Miura, T. (2008) Development of a Two-Band Enhanced Vegetation Index without a Blue Band. *Remote Sensing of Environment*, **112**, 3833-3845. https://doi.org/10.1016/j.rse.2008.06.006

[55] Didan, K. (2014) MOD13Q1: MODIS/Terra Vegetation Indices 16-Day L3 Global 250m Grid SIN V006. NASA EOSDIS Land Processes DAAC, Accessed, **6**.

[56] Oak Ridge National Laboratory (ORNL) Distributed Active Archive Center (DAAC) (2018) MODIS and VIIRS Land Products Global Subsetting and Visualization Tool. Oak Ridge National Laboratory (ORNL) Distributed Active Archive Center (DAAC), Oak Ridge.

[57] Watts, L. and Laffan, S. (2013) Sensitivity of the BFAST Algorithm to MODIS Satellite and Vegetation Index. 20*th International Congress on Modelling and Simulation*. Modelling and Simulation Society of Australia and New Zealand Inc., Adelaide.

[58] Cai, D., Ge, Q., Wang, X., Liu, B., Goudie, A.S. and Hu, S. (2020) Contributions of Ecological Programs to Vegetation Restoration in Arid and Semiarid China. *Environmental Research Letters*, **15**, Article ID: 114046. https://doi.org/10.1088/1748-9326/abbde9

[59] Sedano, F., Lisboa, S., Duncanson, L., Ribeiro, N., Sitoe, A., Sahajpal, R., Hurtt, G. and Tucker, C. (2020) Monitoring Forest Degradation from Charcoal Production with Historical Landsat Imagery. A Case Study in Southern Mozambique. *Environmental Research Letters*, **15**, Article ID: 015001. https://doi.org/10.1088/1748-9326/ab3186

[60] Shi, H., Li, L.H., Eamus, D., *et al.* (2017) Assessing the Ability of MODIS EVI to Estimate Terrestrial Ecosystem Gross Primary Production of Multiple Land Cover Types. *Ecological Indicators*, **72**, 153-164. https://doi.org/10.1016/j.ecolind.2016.08.022

[61] Pan, Y., Li, L., Zhang, J., Liang, S., Zhu, X. and Sulla-Menashe, D. (2012) Winter Wheat Area Estimation from MODIS-EVI Time Series Data Using the Crop Proportion Phenology Index. *Remote Sensing of Environment*, **119**, 232-242. https://doi.org/10.1016/j.rse.2011.10.011

[62] Zhang, J., Feng, L. and Yao, F. (2014) Improved Maize Cultivated Area Estimation Over a Large Scale Combining MODIS–EVI Time Series Data and Crop Phenological Information. *ISPRS Journal of Photogrammetry and Remote Sensing*, **94**, 102-113. https://doi.org/10.1016/j.isprsjprs.2014.04.023

[63] Zhang, X., Sun, R., Zhang, B. and Tong, Q.X. (2008) Land Cover Classification of the North China Plain Using MODIS_EVI Time Series. *ISPRS Journal of Photo-*

grammetry and Remote Sensing, **63**, 476-484.
https://doi.org/10.1016/j.isprsjprs.2008.02.005

[64] Zhang, H.K., Roy, D.P., Yan, L., Li, Z., Huang, H., Vermote, E., Skakun, S. and Roger, J.-C. (2018) Characterization of Sentinel-2A and Landsat-8 Top of Atmosphere, Surface, and Nadir BRDF Adjusted Reflectance and NDVI Differences. *Remote Sensing of Environment*, **215**, 482-494.
https://doi.org/10.1016/j.rse.2018.04.031

[65] Tian, F., Fensholt, R., Verbesselt, J., Grogan, K., Horion, S. and Wang, Y. (2015) Evaluating Temporal Consistency of Long-Term Global NDVI Datasets for Trend Analysis. *Remote Sensing of Environment*, **163**, 326-340.
https://doi.org/10.1016/j.rse.2015.03.031

[66] Myneni, R., Knyazikhin, Y. and Park, T. (2015) MOD15A2H MODIS/Terra Leaf Area Index. FPAR 8-Day L4 Global 500 M SIN Grid V006 Data Set.

[67] Running, S., Mu, Q. and Zhao, M. (2017) Mod16a2 Modis/Terra Net Evapotranspiration 8-Day L4 Global 500m Sin Grid V006. NASA EOSDIS Land Processes DAAC, 6.

[68] Mann, H.B. (1945) Nonparametric Tests against Trend. *Econometrica*: *Journal of the Econometric Society*, **13**, 245-259. https://doi.org/10.2307/1907187

[69] Kendall, K. (1975) Transition between Cohesive and Interfacial Failure in a Laminate. *Proceedings of the Royal Society of London*, *A*: *Mathematical and Physical Sciences*, **344**, 287-302. https://doi.org/10.1098/rspa.1975.0102

[70] Blain, G.C. (2013) Seasonal Variability of Maximum Daily Rainfall in Campinas, State of São Paulo, Brazil: Trends, Periodicities, and Associated Probabilities. *Acta Scientiarum*. *Technology*, **35**, 557-564.
https://doi.org/10.4025/actascitechnol.v35i3.16222

[71] Helsel, D.R. and Hirsch, R.M. (1992) Statistical Methods in Water Resources. Vol. 49, Elsevier, Amsterdam.

[72] Allen, I.E. and Seaman, J. (2010) Class Differences: Online Education in the United States, 2010. Sloan Consortium (NJ1), Needham.

[73] Liu, Y.Y., van Dijk, A.I.J.M., McCabe, M.F., Evans, J.P. and de Jeu, R.A.M. (2013) Global Vegetation Biomass Change (1988-2008) and Attribution to Environmental and Human Drivers. *Global Ecology and Biogeography*, **22**, 692-705. https://doi.org/10.1111/geb.12024

[74] Jiang, Z., Huete, A.R., Kim, Y. and Didan, K. (2007) 2-Band Enhanced Vegetation Index without a Blue Band and Its Application to AVHRR Data. *Remote Sensing and Modeling of Ecosystems for Sustainability IV*, San Diego, 28-29 August 2007, Article ID: 667905. https://doi.org/10.1117/12.734933

[75] Verbesselt, J., Hyndman, R., Zeileis, A. and Culvenora, D. (2010) Phenological Change Detection While Accounting for Abrupt and Gradual Trends in Satellite Image Time Series. *Remote Sensing of Environment*, **114**, 2970-2980.
https://doi.org/10.1016/j.rse.2010.08.003

[76] Lu, J., Carbone, G.J. and Gao, P. (2019) Mapping the Agricultural Drought Based on the Long-Term AVHRR NDVI and North American Regional Reanalysis (NARR) in the United States, 1981-2013. *Applied Geography*, **104**, 10-20.
https://doi.org/10.1016/j.apgeog.2019.01.005

[77] Lu, M., *Chen, J., Tang, H.J., et al.* (2016) Land Cover Change Detection By Integrating Object-Based Data Blending Model of Landsat and MODIS. *Remote Sensing of Environment*, **184**, 374-386. https://doi.org/10.1016/j.rse.2016.07.028

[78] Scholes, M., Martin, R., Scholes, R., Parsons, D. and Winstead, E. (1997) NO and

N_2O Emissions from Savanna Soils Following the First Simulated Rains of the Season. *Nutrient Cycling in Agroecosystems*, **48**, 115-122. https://doi.org/10.1023/A:1009781420199

[79] Sankaran, M., Hanan, N.P., Scholes, R.J., Ratnam, J., Augustine, D.J., Cade, B.S., Gignoux, J., Higgins, S.I., Le Roux, X. and Ludwig, F. (2005) Determinants of Woody Cover in African Savannas. *Nature*, **438**, 846-849. https://doi.org/10.1038/nature04070

[80] Hill, P.G., Allan, R.P., Chiu, J.Y.C. and Stein, T.H.M. (2016) A Multisatellite Climatology of Clouds, Radiation, and Precipitation in Southern West Africa and Comparison to Climate Models. *Journal of Geophysical Research*: *Atmospheres*, **121**, 10,857-10,879. https://doi.org/10.1002/2016JD025246

[81] Cho, H.O., Son, S.W. and Park, D.S.R. (2018) Springtime Extra-Tropical Cyclones in Northeast Asia and Their Impacts on Long-Term Precipitation Trends. *International Journal of Climatology*, **38**, 4043-4050. https://doi.org/10.1002/joc.5543

[82] Higgins, R., Kousky, V. and Xie, P. (2011) Extreme Precipitation Events in the South-Central United States during May and June 2010: Historical Perspective, Role of ENSO, and Trends. *Journal of Hydrometeorology*, **12**, 1056-1070. https://doi.org/10.1175/JHM-D-10-05039.1

[83] Chérif, S. (2014) Construire la résilience au changement climatique par les connaissances locales: Le cas des régions montagneuses et des savanes de Côte d'Ivoire.

[84] Brou, Y.T., Akindès, F. and Bigot, S. (2005) La variabilité climatique en Côte d'Ivoire: Entre perceptions sociales et réponses agricoles. *Cahiers Agricultures*, **14**, 533-540.

[85] Goula, B.T.A., Soro, E.M., Kouassi, W. and Srohourou, B. (2012) Tendances et ruptures au niveau des pluies journalières extrêmes en Côte d'Ivoire (Afrique de l'Ouest). *Hydrological Sciences Journal*, **57**, 1067-1080. https://doi.org/10.1080/02626667.2012.692880

[86] Yoshida, S. (1979) A Simple Evapotranspiration Model of a Paddy Field in Tropical Asia. *Soil Science and Plant Nutrition*, **25**, 81-91. https://doi.org/10.1080/00380768.1979.10433148

[87] Graham, D. and Chapman, E. (1979) Interactions between Photosynthesis and Respiration in Higher Plants. In: Gibbs, M. and Latzko, E., Eds., *Photosynthesis II*, Springer, Berlin, Heidelberg, 150-162. https://doi.org/10.1007/978-3-642-67242-2_12

[88] Zak, D.R., Pregitzer, K.S., Curtis, P.S., *et al.* (1993) Elevated Atmospheric CO_2 and Feedback between Carbon and Nitrogen Cycles. *Plant and Soil*, **151**, 105-117. https://doi.org/10.1007/BF00010791

[89] Yoshida, S. (1978) Tropical Climate and Its Influence on Rice. International Rice Research Institute, Los Banos.

[90] Gang, C., Wang, Z., Chen, Y., Yang, Y., Li, J., Cheng, J., Qi, J. and Odeh, I. (2016) Drought-Induced Dynamics of Carbon and Water Use Efficiency of Global Grasslands from 2000 to 2011. *Ecological Indicators*, **67**, 788-797. https://doi.org/10.1016/j.ecolind.2016.03.049

[91] Gang, H., Li, R., Zhao, Y., Liu, G., Chen, S. and Jiang, J. (2019) Loss of GLK1 Transcription Factor Function Reveals New Insights in Chlorophyll Biosynthesis and Chloroplast Development. *Journal of Experimental Botany*, **70**, 3125-3138. https://doi.org/10.1093/jxb/erz128

[92] Kumarathunge, D.P., Medlyn, B.E., Drake, J.E., Tjoelker, M.G., Aspinwall, M.J., Battaglia, M., Cano, F.J., Carter, K.R., Cavaleri, M.A. and Cernusak, L.A. (2019) Acclimation and Adaptation Components of the Temperature Dependence of Plant Photosynthesis at the Global Scale. *New Phytologist*, **222**, 768-784.

https://doi.org/10.1111/nph.15668

[93] Linthicum, K.J., Anyamba, A., Tucker, C.J., Kelley, P.W., Myers, M.F. and Peters, C.J. (1999) Climate and Satellite Indicators to Forecast Rift Valley Fever Epidemics in Kenya. *Science*, **285**, 397-400. https://doi.org/10.1126/science.285.5426.397

[94] Lotsch, A., Friedl, M.A., Anderson, B.T. and Tucker, C.J. (2005) Response of Terrestrial Ecosystems to Recent Northern Hemispheric Drought. *Geophysical Research Letters*, **32**, Article ID: L06705. https://doi.org/10.1029/2004GL022043

[95] Tucker, C.J., Pinzon, J.E., Brown, M.E., Slayback, D.A., Pak, E.W., Mahoney, R., Vermote, E.F. and El Saleous, N. (2005) An Extended AVHRR 8-Km NDVI Dataset Compatible with MODIS and SPOT Vegetation NDVI Data. *International Journal of Remote Sensing*, **26**, 4485-4498. https://doi.org/10.1080/01431160500168686

[96] Jacques, P., Lambrecht, S., Verheugen, E., Pauwels, E., Kollias, G., Armaka, M., Verhoye, M., Van der Linden, A., Achten, R. and Lories, R.J. (2014) Proof of Concept: Enthesitis and New Bone Formation in Spondyloarthritis Are Driven by Mechanical Strain and Stromal Cells. *Annals of the Rheumatic Diseases*, **73**, 437-445. https://doi.org/10.1136/annrheumdis-2013-203643

[97] Andrew, M.E. and Warrener, H. (2017) Detecting Microrefugia in Semi-Arid Landscapes from Remotely Sensed Vegetation Dynamics. *Remote Sensing of Environment*, **200**, 114-124. https://doi.org/10.1016/j.rse.2017.08.005

[98] Ilangakoon, N.T., Glenn, N.F., Dashti, H., Painter, T.H., Mikesell, T.D., Spaete, L. P., Mitchell, J.J. and Shannon, K. (2018) Constraining Plant Functional Types in a Semi-Arid Ecosystem with Waveform Lidar. *Remote Sensing of Environment*, **209**, 497-509. https://doi.org/10.1016/j.rse.2018.02.070

[99] Cao, Y., Wang, N., Tian, H., Guo, J., Wei, Y., Chen, H., Miao, Y., Zou, W., Pan, K. and He, Y. (2018) Perovskite Light-Emitting Diodes Based on Spontaneously Formed Submicrometre-Scale Structures. *Nature*, **562**, 249-253. https://doi.org/10.1038/s41586-018-0576-2

[100] Yang, Y., Zhao, R., Zhang, T., Zhao, K., Xiao, P., Ma, Y., Ajayan, P. M., Shi, G. and Chen, Y. (2018) Graphene-Based Standalone Solar Energy Converter for Water Desalination and Purification. *ACS Nano*, **12**, 829-835. https://doi.org/10.1021/acsnano.7b08196

[101] Nguyen, N.A., Bowland, C.C. and Naskar, A.K. (2018) Mechanical, Thermal, Morphological, and Rheological Characteristics of High Performance 3D-Printing Lignin-Based Composites for Additive Manufacturing Applications. *Data in Brief*, **19**, 936-950. https://doi.org/10.1016/j.dib.2018.05.130

[102] Woodcock, J. and Johnson, M.R. (2019) The Affective Labor and Performance of Live Streaming on Twitch.tv. *Television & New Media*, **20**, 813-823. https://doi.org/10.1177/1527476419851077

[103] Fournier, A. (1990) Phénologie, croissance et production végétales dans quelques savanes d'Afrique de l'Ouest. No. 6, Université de Paris, Paris.

[104] Gautier, L. (1990) Contact forêt-Savane en Côte-D'Ivoire centrale: Évolution du recouvrement ligneux des savanes de la Réserve de Lamto (sud du V-Baoulé). *Candollea*, **45**, 627-641.

[105] Ouattara, D., Kouame, D., Tiebre, M.-S., et al. (2016) Biodiversité végétale et valeur d'usage en zone soudanienne de la Côte d'Ivoire. *International Journal of Biological and Chemical Sciences*, **10**, 1122-1138. https://doi.org/10.4314/ijbcs.v10i3.18

[106] Koffi, K.F. (2019) Impact du feu sur la démographie des Graminées de savane (Lamto, Côte d'Ivoire). Sorbonne Université; Université Nangui Abrogoua (Abidjan).